Published in final edited form as:
Cell. 2010 October 29; 143(3): 430–441. doi:10.1016/j.cell.2010.09.024.

Endophilin functions as a membrane-bending molecule provided by exocytosis

Jihong Bai[1,2], **Zhitao Hu**[1,2], **Jeremy S. Dittman**[3], **Edward C.G. Pym**[1,2], and **Joshua M. Kaplan**[1,2,4]

[1] Department of Molecular Biology, Massachusetts General Hospital, Boston, MA

[2] Department of Neurobiology, Harvard Medical School, Boston, MA

[3] Department of Biochemistry, Weill Cornell Medical College, New York, NY

Summary

Two models have been proposed for Endophilin function in synaptic vesicle (SV) endocytosis. The scaffolding model proposes that Endophilin's SH3 domain recruits essential endocytic proteins whereas the membrane-bending model proposes that the BAR domain induces positively curved membranes. We show that mutations disrupting the scaffolding function do not impair endocytosis, while those disrupting membrane-bending cause significant defects. By anchoring Endophilin to the plasma membrane, we show that Endophilin acts prior to scission to promote endocytosis. Despite acting at the plasma membrane, the majority of Endophilin is targeted to the SV pool. Photoactivation studies suggest that the soluble pool of Endophilin at synapses is provided by unbinding from the adjacent SV pool and that the unbinding rate is regulated by exocytosis. Thus, Endophilin participates in an association-dissociation cycle with SVs that parallels the cycle of exo- and endocytosis. This Endophilin cycle may provide a mechanism for functionally coupling endocytosis and exocytosis.

Highlights

- **A.** Endophilin functions in SV endocytosis as a membrane-bending molecule.
- **B.** Endophilin functions at the plasma membrane, acting prior to scission.
- **C.** Endophilin is bound to the SV pool and RAB-3 promotes Endophilin-SV association.
- **D.** Soluble Endophilin at synapses is provided by SV exocytosis.

Introduction

Neurotransmitter released at synapses is drawn from a pool of recycling synaptic vesicles (SVs). SVs are consumed by exocytosis and are recycled by endocytosis. To maintain a releasable pool of SVs, the rates of exo- and endocytosis must remain in balance. Stimuli

[4]Corresponding author: Joshua M. Kaplan, Ph.D., Department of Molecular Biology, Massachusetts General Hospital, Richard B Simches Research Building, 185 Cambridge Street CPZN 7250, Boston, MA 02114-2790, Tel: 617-726-5900, Fax: 617-726-5949, kaplan@molbio.mgh.harvard.edu.

that increase SV exocytosis rates produce corresponding increases in endocytosis rates whereas endocytosis is arrested following blockade of exocytosis (Dittman and Ryan, 2009). Relatively little is known about how endocytosis is regulated, nor how the competing processes of SV exocytosis and endocytosis are coordinately regulated.

To begin addressing these questions, we focused on the endocytic protein Endophilin. Endophilin is a conserved protein harboring two functional domains: an N-terminal BAR (Bin–Amphiphysin–Rvs) domain and a C-terminal SH3 (Src homology 3) domain. Inactivation of Endophilin produces profound defects in SV endocytosis (Schuske et al., 2003; Verstreken et al., 2002); however, the mechanism by which Endophilin promotes endocytosis has remained controversial.

Several studies suggest that Endophilin acts primarily as a scaffold, recruiting other essential endocytic proteins via its SH3 domain (Dickman et al., 2005; Gad et al., 2000; Ringstad et al., 1999; Schuske et al., 2003; Verstreken et al., 2002; Verstreken et al., 2003). Endophilin's SH3 domain robustly binds to proline-rich-domains (PRDs) in dynamin and synaptojanin. Antibodies or peptides that interfere with Endophilin's SH3-mediated interactions impair SV recycling and cause accumulation of clathrin-coated vesicles at *lamprey* synapses. In flies and worms, mutants lacking Endophilin have decreased synaptic abundance of Synaptojanin (Schuske et al., 2003; Verstreken et al., 2003). Based on these data, Endophilin was proposed to primarily function as a molecular scaffold.

Analysis of Endophilin's BAR domain suggests an alternative model. Recombinant BAR domains bind liposomes and induce positive curvature of their membranes, as evidenced by the conversion of spherical liposomes into elongated tubules (Farsad et al., 2001). The Endophilin BAR domain also alters membrane morphology in transfected cells (Itoh et al., 2005). Based on these data, Endophilin (and potentially all BAR proteins) were proposed to function by bending membranes. Crystallographic studies suggested a potential mechanism for the Endophilin membrane-bending activity (Gallop et al., 2006; Masuda et al., 2006). Homodimers of the Endophilin BAR domain form a concave membrane binding surface, and specific hydrophobic residues in the BAR domain are proposed to insert into the outer membrane leaflet. Both of these features are predicted to promote positive membrane curvature. While these studies clearly demonstrate Endophilin's membrane-bending ability, whether this activity is required for its endocytic function has not been tested. Although all BAR domains share these *in vitro* membrane bending activities, each BAR protein regulates distinct steps in membrane trafficking. Relatively little is known about how BAR proteins are specifically targeted to distinct membrane trafficking events.

Here we examine the functional importance of the scaffolding and membrane bending activities of Endophilin. We show that the membrane-bending activity is essential for Endophilin's function and that Endophilin undergoes an association-dissociation cycle with SVs that parallels the cycle of exo- and endocytosis. We propose that this Endophilin cycle provides an activity dependent mechanism for delivering Endophilin to endocytic zones.

Results

Endophilin function requires the BAR domain but not the SH3 domain

Due to their endocytosis defects, *unc-57* Endophilin mutants have a smaller pool of SVs and a corresponding decrease in synaptic transmission (Schuske et al., 2003). We exploited three *unc-57* mutant phenotypes as *in vivo* assays of Endophilin function. First, *unc-57* mutants had decreased locomotion rates (Fig. 1A–B; wt 147 ± 9 μm/sec, *unc-57* 33 ± 3 μm/sec, $p<0.001$). Second, *unc-57* mutants had a decreased rate of excitatory post-synaptic currents (EPSCs) at body muscle NMJs (Fig. 1C–D; EPSC rates: wt 38 ± 2.1 Hz, *unc-57* 12 ± 0.9

Hz, $p<0.001$). The mean EPSC amplitude was not significantly altered in *unc-57* mutants (Fig. S1A; EPSC amplitudes: wt 22.7 ± 1.4 pA, *unc-57* 20.7 ± 0.6 pA; $p=0.25$). Third, when endocytosis rates are diminished, the SV protein synaptobrevin becomes increasingly trapped in the plasma membrane. We utilized SynaptopHluorin (SpH) to measure changes in surface synaptobrevin (Dittman and Kaplan, 2006). SpH consists of a pH-sensitive GFP tag fused to the extracellular domain of synaptobrevin. In SVs, SpH fluorescence is quenched by the acidic pH of the vesicle lumen. Following SV fusion, SpH fluorescence on the plasma membrane is dequenched (Dittman and Ryan, 2009). Endophilin mutants had an 83% increase in SpH axon fluorescence compared to wild type controls, consistent with a defect in SV endocytosis (Fig. 1E–F).

Using these assays, we tested the importance of the BAR and SH3 domains for Endophilin's function. Full length and truncated UNC-57 proteins were expressed in *unc-57* mutants. Each construct was tagged with mCherry at the C-terminus, to control for differences in transgene expression (Fig. S1B). Quantitative RT-PCR analysis showed that *unc-57* transgenes were expressed at approximately twice the level of the endogenous *unc-57* mRNA (Fig. S1C). Mutant UNC-57 proteins lacking the SH3 domain fully rescued the locomotion, EPSC, and SpH defects (Fig. 1). By contrast, UNC-57 proteins containing a BAR domain mutation that disrupts membrane binding (ΔN, deletion of N-terminal 26 residues; (Gallop et al., 2006)) lacked rescuing activity in all three assays (Fig. 1). Thus, UNC-57 endocytic function requires the membrane-binding BAR domain but does not require the SH3 domain.

Testing the scaffolding model

Although the SH3 domain was not required for rescuing activity (Fig. 1), it remained possible that UNC-57 primarily functions as a scaffold molecule recruiting other endocytic proteins. We did several experiments to further test the scaffolding model. Consistent with prior studies (Schuske et al., 2003;Verstreken et al., 2003), we found that the fluorescence intensity of GFP::UNC-26 Synaptojanin puncta was slightly reduced in the *unc-57* Endophilin mutants (83% wild type level, $p<0.01$) (Fig. S2A–B). Photobleaching experiments demonstrated that approximately 50% of GFP::UNC-26 was immobile in wild type animals and that this immobile fraction was unaltered in either *unc-57* mutants or in mutants rescued with the BAR domain (Fig. S2D–F). Consequently, Synaptojanin must have additional binding partners beyond Endophilin at synapses. Expressing mutant UNC-57 proteins lacking the SH3 domain rescued the *unc-57* endocytic defects but failed to rescue the UNC-26 Synaptojanin localization defects. In fact, rescued animals had less UNC-26 puncta fluorescence than was observed in *unc-57* mutants (50% and 80% wild type levels respectively, $p<0.001$) (Fig. S2A–B). Similarly, expressing a mutant UNC-26 protein lacking the PRD rescued the locomotion defects of *unc-26* mutants (Fig. S2C). These results agree with a prior study showing that mutations preventing the interaction of mouse Synaptojanin and Endophilin caused only modest endocytic defects (Mani et al., 2007). Collectively, these results support the notion that interactions between Endophilin and Synaptojanin do not play an essential role in SV endocytosis, although it remains possible that these interactions regulate endocytosis in some manner. These experiments also suggest that the modest changes in UNC-26 Synaptojanin targeting are unlikely to account for the *unc-57* endocytic defect.

To further address the scaffolding model, we analyzed two additional endocytic proteins. GFP-tagged dynamin (DYN-1::GFP) and the AP2α-subunit (APT-4::GFP) were both localized to diffraction-limited puncta adjacent to presynaptic elements (labeled with mRFP::SNB-1), suggesting these reporters are localized to perisynaptic endocytic zones. DYN-1 and APT-4 puncta intensities were significantly increased in *unc-57* mutants (Fig. S2), indicating increased synaptic abundance when Endophilin was absent. Mislocalization

of DYN-1 in *unc-57* mutants could arise from the absence of DYN-1 interactions with the UNC-57 SH3. Contrary to this idea, expression of mutant UNC-57 proteins lacking the SH3 corrected the DYN-1 puncta defects, whereas those carrying mutations that prevent membrane binding (ΔN) abolished rescuing activity. These data suggest that the increased synaptic recruitment of DYN-1 and APT-4 observed in *unc-57* mutants is a secondary consequence of the endocytic defect, and do not support a role for Endophilin as a molecular scaffold.

Testing the membrane-bending model

To test the membrane-bending model, we analyzed mutations that disrupt various aspects of BAR domain function *in vitro*. For these experiments, we used the BAR domain derived from rat Endophilin A1 (rEndoA1) because the impact of these mutations on BAR domain activity and structure has only been analyzed for the mammalian proteins. Transgenes were expressed at similar levels (Fig. S3A). Expression of rEndoA1 BAR rescued the locomotion, SpH, and EPSC defects of *unc-57* mutants (Fig. 2 and Fig. S3B). Mutations disrupting membrane binding [rEndoA1 BAR(ΔN)] failed to rescue both the locomotion and SpH defects of *unc-57* mutants (data not shown), consistent with the results we obtained with the UNC-57(ΔN) mutant. These results indicate that the rEndoA1 BAR domain retains endocytic function in *C. elegans* neurons.

Endophilin's tubulation activity *in vitro* is diminished by mutations that prevent dimerization of the BAR domain (ΔH1I), and by mutations that replace hydrophobic residues in the H1 helix with polar residues (M70S/I71S double mutant) (Gallop et al., 2006). Conversely, membrane-bending activity is enhanced by a mutation that increases hydrophobicity of the H1 helix (A66W) (Masuda et al., 2006). Due to its increased membrane bending activity, the A66W protein also lacks tubulation activity, and instead promotes vesiculation of liposomes. None of these mutations significantly alter the membrane binding activity of the BAR domain *in vitro* (Gallop et al., 2006; Masuda et al., 2006).

Transgenes encoding mutant rEndoA1 BAR domains were expressed in *unc-57* mutants. Both the dimerization mutant (ΔH1I) and the tubulation defective mutant (M70S/I71S) had significantly less rescuing activity for the *unc-57* locomotion, SpH, and EPSC rate defects compared to the wild type rEndoA1 BAR domain (Fig. 2 and Fig. S3B). Interestingly, the A66W mutant (which has enhanced membrane-bending activity) also exhibited decreased rescuing activity in all three assays (Fig. 2 and Fig. S3B). None of these tubulation mutants significantly altered endogenous EPSC amplitudes (Fig. S3C–D). These results indicate that Endophilin mutations altering membrane tubulation activity produce corresponding defects in SV endocytosis *in vivo*, consistent with the membrane-bending model. These results also suggest that decreased and increased membrane-bending activity are both detrimental to SV endocytosis.

Specificity of the BAR domain

Membrane association and *in vitro* tubulation activities are common features of most if not all BAR domains; however, only a few BAR domain proteins have been implicated in SV endocytosis. Thus, BAR domains must have other features that confer specificity for their corresponding membrane trafficking functions. To test this idea, we analyzed BAR domains derived from two other proteins. The Endophilin B and Amphiphysin BAR domains both have *in vitro* tubulation activity (Farsad et al., 2001; Peter et al., 2004). Nonetheless, neither BAR domain was able to rescue the *unc-57* locomotion defects (Fig. 2D), although both were well expressed and targeted to axons (data not shown). By contrast, efficient rescue

was observed with transgenes expressing rat and lamprey Endophilin A proteins. These results suggest that only Endophilin A BAR domains can promote SV endocytosis.

To compare their functional properties, we expressed the BAR domains derived from the three rat Endophilin A proteins in *unc-57* mutants. The rEndoA1 and A2 BAR domains fully rescued the *unc-57* locomotion defect, while the A3 BAR domain had significantly less rescuing activity (Fig. 2F). Comparing the H1 helix sequence of these isoforms suggested an explanation for this discrepancy. The rEndoA3 H1 helix contains a hydrophobic tyrosine residue at position 64 while the corresponding residue in the A1 and A2 isoforms is serine (Fig. 2E). An rEndoA3(Y64S) transgene had significantly improved rescuing activity for the *unc-57* locomotion defect (Fig. 2F). These results suggest that sequence differences in the H1 helix contribute to the functional specificity of BAR domains.

Endophilin is targeted to the SV pool

To further examine how Endophilin functions in endocytosis, we analyzed where Endophilin is localized in presynaptic elements. For these experiments, we utilized an UNC-57 construct (UNC-57::CpG) containing two fluorophores, mCherry and photo-activatable GFP (PAGFP). Expressing UNC-57::CpG in all neurons (with the *snb-1* promoter) efficiently rescued the *unc-57* locomotion defect (data not shown), suggesting that this chimeric protein was functional.

UNC-57::CpG was highly enriched at synapses (synapse/axon ratio = 8.6 ± 0.6; n = 38; Fig. 3 and Fig. 4E–F). UNC-57 fluorescence co-localized with two SV markers, GFP::SNB-1 (synaptobrevin) and GFP::RAB-3 (Fig. 3A and Fig. S4A). By contrast, the majority of UNC-57 fluorescence did not colocalize with the endocytic markers APT-4::GFP and DYN-1::GFP (Fig. 3B and data not shown). Thus, at steady state, the majority of UNC-57 was targeted to the SV pool. This conclusion is consistent with prior studies suggesting that Endophilin co-fractionates with SVs in biochemical purifications and that anti-Endophilin antibodies labeled SVs in immunoelectron micrographs (Fabian-Fine et al., 2003;Takamori et al., 2006).

To further investigate how UNC-57 associates with the SV pool, we analyzed *unc-104* KIF1A mutants. In *unc-104* mutants, anterograde transport of SV precursors is defective, resulting in a dramatic decrease in the abundance of SVs at synapses, and a corresponding increase in the abundance of SVs in neuronal cell bodies (Hall and Hedgecock, 1991). We found a similar shift in UNC-57 abundance from axons to cell bodies in *unc-104* mutants (Fig. 3C), consistent with prior studies (Schuske et al., 2003). These results suggest that UNC-57 and SV precursors are co-transported to synapses by UNC-104 KIF1A, as would be expected if UNC-57 were associated with SV precursors. The UNC-57 targeting defect in *unc-104* mutants is unlikely to be a secondary consequence of an underlying defect in active zone assembly, as targeting of several active zone proteins was unaltered in the *unc-104* mutants (Kohn et al., 2000; Koushika et al., 2001). Taken together, these results support the idea that the majority of UNC-57 is targeted to SVs, despite the fact that Endophilin functions at endocytic zones (which are lateral to the SV pool).

Given the preceding results, we would expect that the SV pool contains binding sites that retain UNC-57. To test this idea, we analyzed UNC-57::CpG dispersion following photoactivation at individual synapses (Fig. 4A–D). Photoactivated synaptic UNC-57 rapidly dispersed into the axon (τ = 28.1 ± 3.3 sec; n = 22), while the mCherry signal was unaltered. Mobile photoactivated UNC-57 was rapidly re-captured at adjacent synapses (Fig. S4B). Photoactivated UNC-57 was not observed in axons between synapses, presumably because our imaging rate (1 frame/sec; Fig. S4B) was not fast enough to detect the diffusion of mobile UNC-57. Although we could not directly measure its diffusion rate, these results

suggest that UNC-57 released from the SV pool diffuses as a soluble cytoplasmic protein (which would have a predicted $\tau \sim 140$ msec).

A prior study showed that a sub-population of SVs are mobile, and can be shared between adjacent synapses (Darcy et al., 2006). Three results suggest that dispersion of UNC-57::CpG is unlikely to reflect mobility of SVs bound to UNC-57: (1) photorecovery of an SV marker (GFP::RAB-3) was much slower than that of UNC-57::GFP (Fig. S4C); (2) given the slow mobility of SVs, if the mobile fraction of UNC-57 remained bound to SVs, we should have detected dispersion of photoactivated UNC-57 in axons between synapses; and (3) a small fraction of SVs (2–4%) are mobile in cultured neurons (Darcy et al., 2006; Jordan et al., 2005), whereas 60% of UNC-57 was exchanged in 25 seconds (as measured by both photoactivation and FRAP) (Fig. 4C and Fig. S4D). These data indicate that SV mobility cannot account for the dispersion of photoactivated UNC-57 and instead support the idea that dispersion is mediated by unbinding of UNC-57 from the SV pool.

Exocytosis regulates Endophilin binding to the SV pool

Because Endophilin is targeted to the SV pool, it is possible that Endophilin is delivered to endocytic zones by exocytosis. If this were the case, we would expect that mutations altering exocytosis rates would also alter UNC-57 recruitment to synapses. Consistent with this idea, UNC-57 puncta fluorescence was significantly increased in both *unc-18* Munc18 and *unc-13* Munc13 mutants (12% and 1% wild type EPSC rates, respectively) (Madison et al., 2005; Weimer et al., 2003) (Fig. 4E–F). Thus, decreased SV exocytosis was accompanied by increased UNC-57 synaptic abundance. By contrast, the *tom-1* Tomosyn mutation increases SV exocytosis (McEwen et al., 2006), and caused a parallel decrease in UNC-57 puncta fluorescence (data not shown). Double mutants lacking both UNC-13 and TOM-1 had intermediate SV fusion rates (McEwen et al., 2006) and UNC-57 synaptic abundance values that were intermediate to those observed in either single mutant (Fig. 4F). These results show that bidirectional changes in exocytosis rate produce opposite changes in UNC-57 synaptic enrichment.

If exocytosis regulates UNC-57 targeting by altering binding to the SV pool, exocytosis mutants should also alter the kinetics of UNC-57 dispersion following photoactivation. Consistent with this idea, dispersion rates were significantly reduced in *unc-13* ($\tau = 117.2 \pm 13.6$ sec; n= 20; $p<0.001$) and *unc-18* ($\tau=136.2 \pm 26.4$ sec; n=12, $p<0.001$) mutants compared to wild type controls ($\tau = 28.1 \pm 3.3$ sec; n = 22) (Fig. 4C–D). An intermediate dispersion rate was observed in *tom-1 unc-13* double mutants ($\tau = 68.2 \pm 6.5$ sec, n=18) (Fig. 4D). These results suggest that exocytosis rates regulate UNC-57 dissociation from the SV pool, thereby altering steady-state UNC-57 synaptic abundance.

The exocytosis mutants utilized for these experiments produce global changes in synaptic transmission at all synapses. Consequently, changes in UNC-57 targeting at one synapse may be caused by altered secretion at other synapses. To address this possibility, we inhibited exocytosis in a single class of cholinergic neurons (the DA neurons) by expressing a dominant negative syntaxin mutant. Prior studies showed that increasing the length of the linker between the transmembrane domain and the SNARE helix of Syntaxin inhibits SNARE mediated liposome fusion, presumably because the longer juxtamembrane domain prevents close approximation of the donor and target membranes (McNew et al., 1999). Transgenes expressing Tall Syntaxin in the DA neurons significantly increased synaptic UNC-57 abundance (16.4 ± 1.0; $p<0.001$) and decreased the UNC-57 dispersion rate ($\tau = 49.1 \pm 3.3$ sec; $p<0.001$) compared to wild type controls (synapse/axon ratio = 8.6 ± 0.6 and $\tau = 28.1 \pm 3.3$ sec, respectively) (Fig. S5). These results indicate that changes in exocytosis rates regulate synaptic recruitment of UNC-57 in a cell autonomous manner, as would be expected if exocytosis regulates UNC-57 binding to the SV pool.

Structural requirements for UNC-57 regulation by exocytosis

We did several experiments to determine how UNC-57 senses changes in exocytosis. A mutant UNC-57 protein lacking the SH3 domain (BAR::CpG) rescues the *unc-57* endocytic defects (Fig. 1) and was properly targeted to the SV pool (Fig. S6A). In *unc-13* mutants, the BAR dispersion rate was significantly decreased (wt τ = 32.3 ± 2.8 sec, *unc-13* τ = 122.6 ± 16.7, $p<0.001$) (Fig. 5A). By contrast, a mutation disrupting membrane binding, UNC-57(ΔN), eliminated the effect of *unc-13* mutations on dispersion rates (wt τ = 16.2 ± 3.8 sec, *unc-13* τ = 19.1 ± 1.7 sec, $p=0.49$) (Fig. 5B) and significantly reduced UNC-57 synaptic enrichment (Fig. S6). These results demonstrate that the membrane binding activity of the BAR domain is required for UNC-57 regulation by exocytosis.

We next asked if membrane-bending activity of the BAR domain is required for regulation by exocytosis. The UNC-57(A66W) mutant had increased membrane bending activity *in vitro* and decreased rescuing ability *in vivo*. Nonetheless, the dispersion rates A66W and wild type UNC-57 were indistinguishable, and were slowed to the same extent in *unc-13* mutants (Fig. 5C). Similarly, the dimerization defective UNC-57(ΔH1I) mutant was localized to presynaptic elements (Fig. S6), and its dispersion rate was significantly reduced in *unc-13* mutants (wt τ = 20.5 ± 2.5 sec, *unc-13* τ = 48.5 ± 5.2 sec, $p<0.001$) (Fig. 5D). These data suggest that Endophilin monomers bind to SVs, and that exocytosis stimulates unbinding of monomers from SVs. Thus, membrane-bending activity is not required for UNC-57 binding to the SV pool nor for its regulation by exocytosis.

Although monomeric UNC-57 retained the ability to sense changes in exocytosis, the ΔH1I dispersion rate was significantly faster than that observed for wild type UNC-57 (Fig. 5D) and the ΔH1I synaptic enrichment was also reduced (Fig. S6B). These results suggest that monomeric UNC-57 binds to SVs with lower affinity than UNC-57 dimers.

RAB-3 promotes UNC-57 targeting to the SV pool

If UNC-57 binds directly to SVs, we would expect that a protein associated with SVs would promote its synaptic targeting. Several results suggest that the RAB-3 GTP-binding protein enhances UNC-57 recruitment to the SV pool. To test the role of RAB-3, we analyzed *aex-3* mutants. The *aex-3* gene encodes the GDP/GTP exchange factor for RAB-3 and AEX-6 Rab27 (AEX-3 Rab3 GEF). Mutants lacking AEX-3 have an SV exocytosis defect that is very similar to the defect observed in *rab-3; aex-6* Rab27 double mutants (Mahoney et al., 2006). As in other exocytosis mutants, photoactivated UNC-57 dispersed more slowly in *aex-3* mutants (τ = 45.5 ± 5.1 sec, $p<0.01$; Fig. 6C). Given this reduced UNC-57 dispersion rate, we would expect that *aex-3* mutants would have increased synaptic enrichment of UNC-57. Surprisingly, UNC-57 synaptic enrichment was significantly reduced (28% decrease) in *aex-3* mutants (WT 8.6 ± 0.6, *aex-3* 6.2 ± 0.6, $p<0.01$; Fig. 6A–B), unlike the increased enrichment observed in other exocytosis mutants (e.g. *unc-13* 32.5 ± 2.1). This result is not due to a generalized decrease in the abundance of SV proteins, because *aex-3* mutants had increased SNB-1 synaptobrevin accumulation (38% increase, $p<0.001$) (Ch'ng, 2008). These results suggest that inactivating the AEX-3 Rab3GEF reduced UNC-57 recruitment to the SV pool, but did not prevent exocytosis-dependent regulation of UNC-57 unbinding from the SV pool.

Because *aex-3* mutants also have an exocytosis defect (and consequently a decreased UNC-57 dispersion rate), it is likely that this experiment underestimates the magnitude of the *aex-3* defect in UNC-57 synaptic recruitment. To more accurately assess the role of AEX-3, we analyzed *unc-13; aex-3* double mutants, in which SV exocytosis is nearly completely blocked. UNC-57 synaptic enrichment was significantly reduced in *unc-13; aex-3* double mutants (39% decrease), when compared to *unc-13* single mutants (*unc-13;*

aex-3 19.6 ± 1.2, *unc-13* 32.1 ± 2.2 fold; $p<0.001$; Fig. 6A–B). Thus, changes in exocytosis cannot explain the *aex-3* mutant defect in UNC-57 synaptic recruitment. Instead, these results support the idea that AEX-3 promotes UNC-57 recruitment to the SV pool.

We next asked if the AEX-3 substrate RAB-3 regulates UNC-57 targeting. In *aex-3* mutants, RAB-3 is absent from axons and accumulates in neuronal cell bodies (Mahoney et al., 2006). Therefore, defects in UNC-57 targeting could arise from either lack of axonal RAB-3 or from mis-regulation of RAB-3 GTP/GDP cycle. Expression of a GTP-locked (Q81L) form of RAB-3 significantly reduced UNC-57::CpG synaptic accumulation in *unc-13* mutants (Fig. 6D–E). In contrast, the GDP-locked (T36N) form of RAB-3 had no effect on UNC-57 enrichment. Taken together, these data suggest that AEX-3 and RAB-3·GTP regulate UNC-57 targeting to the SV pool, even when exocytosis is blocked.

A plasma membrane-anchored Endophilin is targeted to endocytic zones

unc-57 mutants accumulate coated membranes, and invaginated coated pits (Schuske et al., 2003). Based on these studies, Endophilin has been variously proposed to act before scission, or to promote uncoating of endocytic vesicles after scission. Our preceding results suggest a third possibility. Endophilin may also act prior to fusion, i.e. bound to SVs. To distinguish between these possibilities, we designed a mutant form of Endophilin that is constitutively bound to the plasma membrane [UNC-57(PM)]. UNC-57(PM) contains full length UNC-57 and GFP fused to the N-terminus of the plasma membrane protein UNC-64/Syntaxin1A (Fig. S7A). To control for the impact of Syntaxin's cytoplasmic domains on UNC-57(PM), we also analyzed a deletion mutant lacking the Syntaxin membrane spanning domain, termed UNC-57(Cyto).

We analyzed the subcellular distribution of UNC-57 when it is constitutively anchored to the plasma membrane. Unlike UNC-64/Syntaxin1A, which has a diffuse distribution on plasma membranes (Fig. S7B), UNC-57(PM) was highly enriched in synaptic puncta (Fig. 7). Although UNC-57(PM) and wild type UNC-57 were both punctate, their properties differed in several respects. UNC-57(PM) puncta were significantly smaller than UNC-57 puncta (Fig. 7A; puncta width: UNC-57(PM): 0.51 ± 0.02 μm, n=28; UNC-57: 0.75 ± 0.02 μm, n=38; $p<0.001$). Furthermore, a majority of the UNC-57(PM) fluorescence was colocalized with the endocytic marker APT-4::GFP, while far less colocalization was observed with SV pool, labeled with either wild type UNC-57::CpG (Fig. 7) or mcherry::RAB-3 (data not shown). By contrast, wild type UNC-57 had the converse pattern, exhibiting greater colocalization with the SV pool than with endocytic zones (Fig. 3 and Fig. S4A).

Because UNC-57(PM) and APT-4 puncta are both diffraction limited, it remained possible that these proteins are localized to distinct presynaptic subdomains that cannot be resolved by conventional confocal microscopy. We did several experiments to control for this possibility. First, UNC-57(PM) is unlikely to be targeted to active zones, as it failed to colocalize with the active zone marker ELKS-1 (Fig. 7A). Second, if UNC-57(PM) is targeted to endocytic zones, then it should behave like other endocytic zone proteins. We previously showed that *unc-13* mutations have opposite effects on the synaptic abundance of SV proteins (increasing SNB-1 and RAB-3) versus endocytic proteins (decreasing APT-4 AP2α) (Ch'ng et al., 2008;Dittman and Kaplan, 2006). The reduced targeting of APT-4 to endocytic zones is presumably caused by the decreased abundance of SV cargo in the plasma membrane when exocytosis is blocked (Dittman and Kaplan, 2006). UNC-57(PM) puncta fluorescence was significantly decreased (42 ± 3% reduction, $p<0.001$) in *unc-13* mutants (Fig. 7B), which is similar to the behavior of APT-4 (21% decrease, $p<0.001$), and opposite to the behavior of RAB-3 (26% increase, $p<0.01$) (Ch'ng et al., 2008). Thus, when exocytosis is blocked, UNC-57(PM) behaves like an endocytic protein and not like an SV-associated protein. In contrast, a membrane-anchored BAR domain [BAR(PM)], lacking the

SH3 domain, had a diffuse axonal distribution similar to UNC-64 Syntaxin (Fig. 7C). UNC-57(Cyto), which lacks the Syntaxin transmembrane domain, behaved similarly to wild type UNC-57 and other SV proteins, i.e., its synaptic abundance was increased in *unc-13* mutants (Fig. S7C). Thus, the membrane-spanning domain anchors UNC-57(PM) to the plasma membrane, preventing its association with the SV pool. Once anchored in the plasma membrane, the SH3 domain promotes UNC-57 targeting to endocytic zones.

UNC-57(PM) rescues the endocytic defects of *unc-57* mutants

To determine if UNC-57 functions on the plasma membrane, we assayed the ability of UNC-57(PM) rescue the synaptic defects of *unc-57* mutants. The UNC-57(PM) transgene rescued the *unc-57* mutant locomotion and endogenous EPSC rate defects (Fig. 7D–E). Thus, a plasma membrane-anchored form of UNC-57 retains the ability to promote endocytosis. These results suggest that UNC-57 promotes endocytosis by regulating a step that occurs prior to both scission and uncoating of endocytic vesicles. Interestingly, the membrane-anchored UNC-57(PM) protein had significantly less rescuing activity than the UNC-57(Cyto) construct, which lacks the Syntaxin membrane spanning domain (Fig. S7D–F). This discrepancy suggests that the membrane-tethered protein can not fully reconstitute UNC-57's endocytic function. For example, UNC-57's endocytic activity may be more potent when it is delivered via association with SVs. Alternatively, UNC-57 Endophilin may have additional functions that occur after scission.

Does membrane anchoring of UNC-57 bypass the requirement for direct interactions between membranes and the BAR domain? Contrary to this idea, an UNC-57(PM) transgene containing the ΔN mutation failed to rescue the *unc-57* mutant synaptic defects (Fig. 7D–E), although this mutant protein was efficiently targeted to synaptic puncta (Fig. 7C). The BAR(PM) protein, which lacks the SH3 domain, had a diffuse axonal distribution (Fig. 7C) yet rescued the EPSC defect to an equivalent level as the UNC-57(PM) protein (Fig. 7D–E). Thus, a diffusely distributed membrane-anchored BAR domain was sufficient to support SV endocytosis (Fig. 7D–E). Interestingly, endogenous EPSC amplitudes were significantly larger in animals expressing BAR(PM) compared to those observed in animals expressing UNC-57(PM) (p=0.018; Fig. 7D–E), suggesting that SV recycling had been subtly altered by removing the SH3 domain.

Discussion

Our results lead to six primary conclusions. First, Endophilin promotes SV endocytosis by acting as a membrane-bending molecule, not as a molecular scaffold. Second, Endophilin functions on the plasma membrane, promoting an early step in endocytosis (prior to scission of endocytic vesicles). Third, Endophilin A BAR domains are specialized to promote SV endocytosis. Fourth, Endophilin is targeted to synapses by its association with the SV pool. Fifth, RAB-3 promotes Endophilin association with the SV pool. And sixth, Endophilin dissociation from the SV pool is regulated by exocytosis. Collectively, these results argue that Endophilin undergoes a membrane association/dissociation cycle that parallels the SV cycle. Below we discuss the implications of these results for understanding SV endocytosis.

Endophilin function as a molecular scaffold

Prior studies proposed that Endophilin primarily functions as a scaffolding molecule, recruiting other endocytic proteins via its SH3 domain (Dickman et al., 2005; Gad et al., 2000; Ringstad et al., 1999; Schuske et al., 2003; Verstreken et al., 2002; Verstreken et al., 2003). Consistent with these studies, we find that Synaptojanin abundance at synapses was modestly reduced while DYN-1 and APT-4 AP2α abundance were increased in *unc-57* mutants. Several results argue against the idea that this putative scaffolding function

constitutes Endophilin's major role in endocytosis. Deleting the SH3 domain did not impair the endocytic function of UNC-57. Similarly, deleting the PRD did not impair synaptojanin's endocytic function, which agrees with analogous experiments analyzing mouse synaptojanin (Mani et al., 2007). Finally, changes in synaptojanin and dynamin targeting did not correlate with rescue of the *unc-57* endocytic defects. Thus, altered recruitment of endocytic molecules is unlikely to account for the endocytic defects of *unc-57* mutants. Instead, these localization defects are more likely a secondary consequence of the endocytic defects.

What is Endophilin's function in endocytosis?

Beyond scaffolding, several other mechanisms have been proposed for Endophilin's endocytic function, including promoting early steps (prior to scission) and later steps (e.g. uncoating of endocytosed vesicles). Our results indicate that Endophilin acts at the plasma membrane and consequently must function prior to scission. An Endophilin mutant that is permanently anchored to the plasma membrane [UNC-57(PM)] reconstitutes SV endocytosis when expressed in *unc-57* mutants. UNC-57(PM) remains in the plasma membrane, and does not equilibrate into the recycled SV pool. Thus, at least one aspect of Endophilin function can be executed at the plasma membrane. Our results do not exclude the possibility that Endophilin also has a later function.

Our analysis suggests that the BAR domain, and its membrane bending activity, plays the primary and essential function of Endophilin in SV endocytosis. The curvature inducing activity of Endophilin could promote internalization of cargo from the plasma membrane. Consistent with this idea, the membrane-anchored UNC-57(PM) protein was highly enriched at endocytic zones. A prior study showed that Endophilin accumulates along the neck of plasma membrane invaginations following inactivation of dynamin, also consistent with Endophilin acting prior to scission (Ferguson et al., 2009). Alternatively, the membrane-bending function of the BAR domain could act following scission, perhaps by accelerating vesicle uncoating.

The SH3 domain is conserved in all Endophilin proteins, implying that it plays an important role. Although not essential for endocytosis, several results indicate that the SH3 domain regulates Endophilin's activity in certain contexts. Once anchored to the plasma membrane, the SH3 domain targeted UNC-57 to endocytic zones, presumably via interactions with dynamin or synaptojanin. Although membrane-anchored constructs containing and lacking the SH3 domain [UNC-57(PM) and BAR(PM)] rescued the *unc-57* endocytic defects equally well, EPSC amplitudes (a measure of quantal size) were significantly increased by the BAR(PM) transgene. In principle, an increased quantal size could be caused by delayed scission, which would produce larger recycled SVs. Alternatively, this defect could arise from faster re-filling of recycled SVs with neurotransmitter (e.g. by increased recycling of VAChT transporters). Whatever the mechanism involved, our results suggest that Endophilin alters quantal size only in specific circumstances, as EPSC amplitudes were not altered in *unc-57* null mutants. Similarly, at the *Drosophila* larval NMJ, Endophilin's effect on quantal size varied depending on the stimulus rate (Dickman et al., 2005). Collectively, these results are most consistent with the idea that Endophilin has multiple functions at the plasma membrane, perhaps including both internalization of endocytic cargo and adjusting the timing of membrane scission.

BAR domain specificity

Membrane-bending activity is a shared feature of most (perhaps all) BAR proteins (Peter et al., 2004); however, only two BAR proteins (Endophilin and Amphiphysin) have been implicated in SV endocytosis. This suggests that BAR domains contain other determinants

that confer specificity for distinct membranes and trafficking functions. In support of this idea, BAR domains derived from Endophilin B and Amphiphysin did not rescue *unc-57* endocytic defects whereas those derived from several Endophilin A proteins did rescue. The endocytic function of rat Endophilin A1 and A3 BAR domains differed significantly, due to a sequence difference in the H1 helix. Thus, the H1 helix may confer functional specificity to BAR domains.

Endophilin is targeted to the SV pool

Although Endophilin functions at endocytic zones, our results suggest that that 90% of Endophilin at presynaptic sites is bound to the SV pool, while the remainder has a diffuse axonal distribution. We propose that UNC-57 association with SVs is mediated by at least two factors: direct binding of the BAR domain to the SV membrane (disrupted by the ΔN mutant) and a second RAB-3 dependent mode of SV binding (disrupted in *aex-3* Rab3 GEF mutants). The RAB-3 effect is likely mediated by the GTP-bound form of RAB-3 and is independent of RAB-3's effect on SV exocytosis. Further study is needed to determine if this is mediated by direct binding of RAB-3 to UNC-57. Prior studies also support Endophilin's association with the SV pool (Fabian-Fine et al., 2003; Takamori et al., 2006).

SV exocytosis provides soluble Endophilin at synapses

Our results suggest that Endophilin undergoes an association/dissociation cycle with SVs, and that dissociation from SVs is stimulated by exocytosis. By analyzing a panel of mutants with a range of exocytosis rates, we observed that the rate of UNC-57 dispersion (or unbinding from the SV pool) was positively correlated with the exocytosis rate. A mutant UNC-57 lacking membrane binding activity (ΔN) was not regulated by the exocytosis rate, suggesting that binding of UNC-57 to SVs is required to sense exocytosis. By contrast, neither tubulation defective mutants nor dimerization mutants prevented UNC-57 regulation by exocytosis. Thus, distinct biochemical properties of Endophilin are required for binding to SVs, sensing exocytosis, and promoting endocytosis. A consequence of this mechanism for regulating Endophilin availability is that proteins previously thought to act solely during SV exocytosis (e.g. RAB-3 and AEX-3 Rab3 GEF), also have the potential to regulate endocytosis.

Implications for regulating SV endocytosis

SV endocytosis is tightly coupled to exocytosis, which allows neurotransmission to be sustained and presynaptic membrane turnover to remain balanced. To date, the mechanism underlying coupling of SV exo- and endocytosis is not well understood. Two general models have been proposed. First, changes in presynaptic calcium could potentially produce coordinated changes in exo- and endocytosis, as calcium potently regulates both processes (Dittman and Ryan, 2009). A recent publication proposed a second model, whereby rate limiting endocytic proteins are delivered to endocytic zones by associating with SVs (Shupliakov, 2009). For example, the endocytic proteins intersectin and EPS15 were previously shown to associate with the SV pool in resting synapses, but both are dynamically recruited to endocytic zones following depolarization (Shupliakov, 2009).

Consistent with the latter model, we propose that wild type UNC-57 is delivered to synapses via its association with SVs, that the endocytic pool of UNC-57 is provided by unbinding from the adjacent SV pool, and that UNC-57 delivery to endocytic zones is stimulated by exocytosis. The requirement for SV-mediated delivery can be bypassed by artificially anchoring UNC-57 to the plasma membrane. However, the membrane-anchored protein had diminished rescuing activity, implying that UNC-57's endocytic activity is more potent when delivered via association with SVs.

Several results support this model. Endophilin binds to the SV pool and dissociation from SV's is stimulated by exocytosis. The SV bound pool of UNC-57 is likely to be inactive for several reasons. First, SV binding sequesters Endophilin away from endocytic zones. And second, our results suggest that Endophilin bound to SVs remains in an inactive, monomeric conformation. Upon release from SVs, soluble Endophilin monomers would be free to form active dimers, and to subsequently promote membrane bending at endocytic zones. Because soluble UNC-57 diffuses into the cytosol, we propose that exocytosis would provide a pulse of active Endophilin thereby promoting endocytosis at the adjacent endocytic zone. It is worth noting that such an increase in Endophilin concentration at endocytic zones is transient, i.e. soluble Endophilin concentration rapidly decreases with time and distance, providing a tight temporal and spatial control on exocytosis-endocytosis coupling. Calcium regulation is unlikely to explain our results, as presynaptic Ca^{2+} currents were unaltered in Munc13-1/2 double knockout neurons (Varoqueaux et al., 2002) yet *unc-13* mutations potently regulated UNC-57 unbinding from SVs. It is also possible that both mechanisms act in concert to couple exo- and endocytosis.

Our results also predict that distinct endocytic mechanisms may be employed during stimulus trains, versus those utilized following stimulation. During a stimulus, soluble Endophilin will be continuously provided by ongoing SV exocytosis. By contrast, following a stimulus, exocytosis rates decline, and the concentration of soluble Endophilin will drop dramatically. Thus, we predict that Endophilin does not play an important role in compensatory endocytosis. Indeed, a slow form of SV endocytosis persists in mutant flies lacking Endophilin (Dickman et al., 2005). Prior studies of dynamin-1 knockouts also support the idea that distinct modes of endocytosis occur during versus after stimulus trains (Ferguson et al., 2007). We speculate that delivery of key endocytic proteins by SV exocytosis provides a potential mechanism to explain the different modes of endocytosis that occur at synapses. Because Endophilin potentially functions at multiple steps of the recycling pathway, these modes of endocytosis may differ in several ways (e.g. endocytosis rate, quantal size, and the rate at which recycled SVs become available for re-release).

Experimental Procedures

Strains

A full list of strains is provided in the Supplementary text. Transgenic animals were prepared by microinjection, and integrated transgenes were isolated following UV irradiation, as described (Dittman and Kaplan, 2006).

Constructs

cDNAs of *unc-57* and *erp-1* were amplified from total mRNA extracted from wild type worms. cDNAs of rat endophilin A1, A2, A3, endophlin B1 and amphiphysin were amplified from a cDNA library from Clontech (Mountain View, CA). cDNA of lamprey endophilin was synthesized by Genscript (Piscataway, NJ). All constructs were generated using modified pPD49.26 vectors. A more detailed description of all constructs is provided in the Supplementary text.

In Vivo Microscopy and Image Analysis

Animals were immobilized with 2,3-Butanedione monoxamine (30mg/mL; Sigma-Aldrich), and images were collected with an Olympus FV-1000 confocal microscope with an Olympus PlanApo 60× Oil 1.45 NA objective at 5x zoom, a 488nm Argon laser (GFP), a 559nm diode laser (mCherry), and a 405nm diode laser (photoactivation). Detailed descriptions of the photoactivation protocol and image analysis are provided in the Supplementary Information.

Worm Tracking and Locomotion Analysis

Locomotion behavior of young adult animals (room temperature, off food) was recorded on a Zeiss Discovery Stereomicroscope using Axiovision software. The center of mass was recorded for each animal on each video frame using object tracking software in Axiovision. Imaging began 1 hour after worms were removed from food.

Electrophysiology

Strains for electrophysiology were maintained at 20°C on plates seeded with HB101. Adult worms were immobilized on Sylgard coated coverslips with cyanoacrylate glue. Dissections and whole-cell recordings were carried out as previously described (Madison et al., 2005; Richmond and Jorgensen, 1999). Statistical significance was determined on a worm-by-worm basis using the Mann-Whitney test or student's t-test for comparison of mean frequency and amplitude for endogenous EPSCs.

Supplementary Material

Refer to Web version on PubMed Central for supplementary material.

Acknowledgments

We thank the following for strains and reagents: Roger Tsien, Jennifer Lippincott-Schwartz and the *C. elegans* Genetics Stock Center. We thank members of the Kaplan lab and Susana Garcia for critical comments. This work was supported by a Jane Coffin Childs postdoctoral fellowship (J.B.) and by NIH grants GM54728 (J.K.) and K99MH085039 (J.B.).

References

Ch'ng Q, Sieburth D, Kaplan JM. Profiling synaptic proteins identifies regulators of insulin secretion and lifespan. PLoS Genet. 2008; 4:e1000283. [PubMed: 19043554]

Darcy KJ, Staras K, Collinson LM, Goda Y. Constitutive sharing of recycling synaptic vesicles between presynaptic boutons. Nat Neurosci. 2006; 9:315–321. [PubMed: 16462738]

Dickman DK, Horne JA, Meinertzhagen IA, Schwarz TL. A slowed classical pathway rather than kiss-and-run mediates endocytosis at synapses lacking synaptojanin and endophilin. Cell. 2005; 123:521–533. [PubMed: 16269341]

Dittman J, Ryan TA. Molecular circuitry of endocytosis at nerve terminals. Annu Rev Cell Dev Biol. 2009; 25:133–160. [PubMed: 19575674]

Dittman JS, Kaplan JM. Factors regulating the abundance and localization of synaptobrevin in the plasma membrane. Proc Natl Acad Sci U S A. 2006; 103:11399–11404. [PubMed: 16844789]

Fabian-Fine R, Verstreken P, Hiesinger PR, Horne JA, Kostyleva R, Zhou Y, Bellen HJ, Meinertzhagen IA. Endophilin promotes a late step in endocytosis at glial invaginations in Drosophila photoreceptor terminals. J Neurosci. 2003; 23:10732–10744. [PubMed: 14627659]

Farsad K, Ringstad N, Takei K, Floyd SR, Rose K, De Camilli P. Generation of high curvature membranes mediated by direct endophilin bilayer interactions. J Cell Biol. 2001; 155:193–200. [PubMed: 11604418]

Ferguson SM, Brasnjo G, Hayashi M, Wolfel M, Collesi C, Giovedi S, Raimondi A, Gong LW, Ariel P, Paradise S, et al. A selective activity-dependent requirement for dynamin 1 in synaptic vesicle endocytosis. Science. 2007; 316:570–574. [PubMed: 17463283]

Ferguson SM, Raimondi A, Paradise S, Shen H, Mesaki K, Ferguson A, Destaing O, Ko G, Takasaki J, Cremona O, et al. Coordinated actions of actin and BAR proteins upstream of dynamin at endocytic clathrin-coated pits. Dev Cell. 2009; 17:811–822. [PubMed: 20059951]

Gad H, Ringstad N, Low P, Kjaerulff O, Gustafsson J, Wenk M, Di Paolo G, Nemoto Y, Crun J, Ellisman MH, et al. Fission and uncoating of synaptic clathrin-coated vesicles are perturbed by disruption of interactions with the SH3 domain of endophilin. Neuron. 2000; 27:301–312. [PubMed: 10985350]

Gallop JL, Jao CC, Kent HM, Butler PJ, Evans PR, Langen R, McMahon HT. Mechanism of endophilin N-BAR domain-mediated membrane curvature. EMBO J. 2006; 25:2898–2910. [PubMed: 16763559]

Hall DH, Hedgecock EM. Kinesin-related gene unc-104 is required for axonal transport of synaptic vesicles in C. elegans. Cell. 1991; 65:837–847. [PubMed: 1710172]

Itoh T, Erdmann KS, Roux A, Habermann B, Werner H, De Camilli P. Dynamin and the actin cytoskeleton cooperatively regulate plasma membrane invagination by BAR and F-BAR proteins. Dev Cell. 2005; 9:791–804. [PubMed: 16326391]

Jordan R, Lemke EA, Klingauf J. Visualization of synaptic vesicle movement in intact synaptic boutons using fluorescence fluctuation spectroscopy. Biophys J. 2005; 89:2091–2102. [PubMed: 15980175]

Kohn RE, Duerr JS, McManus JR, Duke A, Rakow TL, Maruyama H, Moulder G, Maruyama IN, Barstead RJ, Rand JB. Expression of multiple UNC-13 proteins in the Caenorhabditis elegans nervous system. Mol Biol Cell. 2000; 11:3441–3452. [PubMed: 11029047]

Koushika SP, Richmond JE, Hadwiger G, Weimer RM, Jorgensen EM, Nonet ML. A post-docking role for active zone protein Rim. Nat Neurosci. 2001; 4:997–1005. [PubMed: 11559854]

Madison JM, Nurrish S, Kaplan JM. UNC-13 interaction with syntaxin is required for synaptic transmission. Curr Biol. 2005; 15:2236–2242. [PubMed: 16271476]

Mahoney TR, Liu Q, Itoh T, Luo S, Hadwiger G, Vincent R, Wang ZW, Fukuda M, Nonet ML. Regulation of synaptic transmission by RAB-3 and RAB-27 in Caenorhabditis elegans. Mol Biol Cell. 2006; 17:2617–2625. [PubMed: 16571673]

Mani M, Lee SY, Lucast L, Cremona O, Di Paolo G, De Camilli P, Ryan TA. The dual phosphatase activity of synaptojanin1 is required for both efficient synaptic vesicle endocytosis and reavailability at nerve terminals. Neuron. 2007; 56:1004–1018. [PubMed: 18093523]

Masuda M, Takeda S, Sone M, Ohki T, Mori H, Kamioka Y, Mochizuki N. Endophilin BAR domain drives membrane curvature by two newly identified structure-based mechanisms. EMBO J. 2006; 25:2889–2897. [PubMed: 16763557]

McEwen JM, Madison JM, Dybbs M, Kaplan JM. Antagonistic regulation of synaptic vesicle priming by Tomosyn and UNC-13. Neuron. 2006; 51:303–315. [PubMed: 16880125]

McNew JA, Weber T, Engelman DM, Sollner TH, Rothman JE. The length of the flexible SNAREpin juxtamembrane region is a critical determinant of SNARE-dependent fusion. Mol Cell. 1999; 4:415–421. [PubMed: 10518222]

Patterson GH, Lippincott-Schwartz J. A photoactivatable GFP for selective photolabeling of proteins and cells. Science. 2002; 297:1873–1877. [PubMed: 12228718]

Peter BJ, Kent HM, Mills IG, Vallis Y, Butler PJ, Evans PR, McMahon HT. BAR domains as sensors of membrane curvature: the amphiphysin BAR structure. Science. 2004; 303:495–499. [PubMed: 14645856]

Richmond JE, Jorgensen EM. One GABA and two acetylcholine receptors function at the C. elegans neuromuscular junction. Nat Neurosci. 1999; 2:791–797. [PubMed: 10461217]

Ringstad N, Gad H, Low P, Di Paolo G, Brodin L, Shupliakov O, De Camilli P. Endophilin/SH3p4 is required for the transition from early to late stages in clathrin-mediated synaptic vesicle endocytosis. Neuron. 1999; 24:143–154. [PubMed: 10677033]

Schuske KR, Richmond JE, Matthies DS, Davis WS, Runz S, Rube DA, van der Bliek AM, Jorgensen EM. Endophilin is required for synaptic vesicle endocytosis by localizing synaptojanin. Neuron. 2003; 40:749–762. [PubMed: 14622579]

Shupliakov O. The synaptic vesicle cluster: a source of endocytic proteins during neurotransmitter release. Neuroscience. 2009; 158:204–210. [PubMed: 18440714]

Takamori S, Holt M, Stenius K, Lemke EA, Gronborg M, Riedel D, Urlaub H, Schenck S, Brugger B, Ringler P, et al. Molecular anatomy of a trafficking organelle. Cell. 2006; 127:831–846. [PubMed: 17110340]

Varoqueaux F, Sigler A, Rhee JS, Brose N, Enk C, Reim K, Rosenmund C. Total arrest of spontaneous and evoked synaptic transmission but normal synaptogenesis in the absence of Munc13-mediated vesicle priming. Proc Natl Acad Sci U S A. 2002; 99:9037–9042. [PubMed: 12070347]

Verstreken P, Kjaerulff O, Lloyd TE, Atkinson R, Zhou Y, Meinertzhagen IA, Bellen HJ. Endophilin mutations block clathrin-mediated endocytosis but not neurotransmitter release. Cell. 2002; 109:101–112. [PubMed: 11955450]

Verstreken P, Koh TW, Schulze KL, Zhai RG, Hiesinger PR, Zhou Y, Mehta SQ, Cao Y, Roos J, Bellen HJ. Synaptojanin is recruited by endophilin to promote synaptic vesicle uncoating. Neuron. 2003; 40:733–748. [PubMed: 14622578]

Weimer RM, Richmond JE, Davis WS, Hadwiger G, Nonet ML, Jorgensen EM. Defects in synaptic vesicle docking in unc-18 mutants. Nat Neurosci. 2003; 6:1023–1030. [PubMed: 12973353]

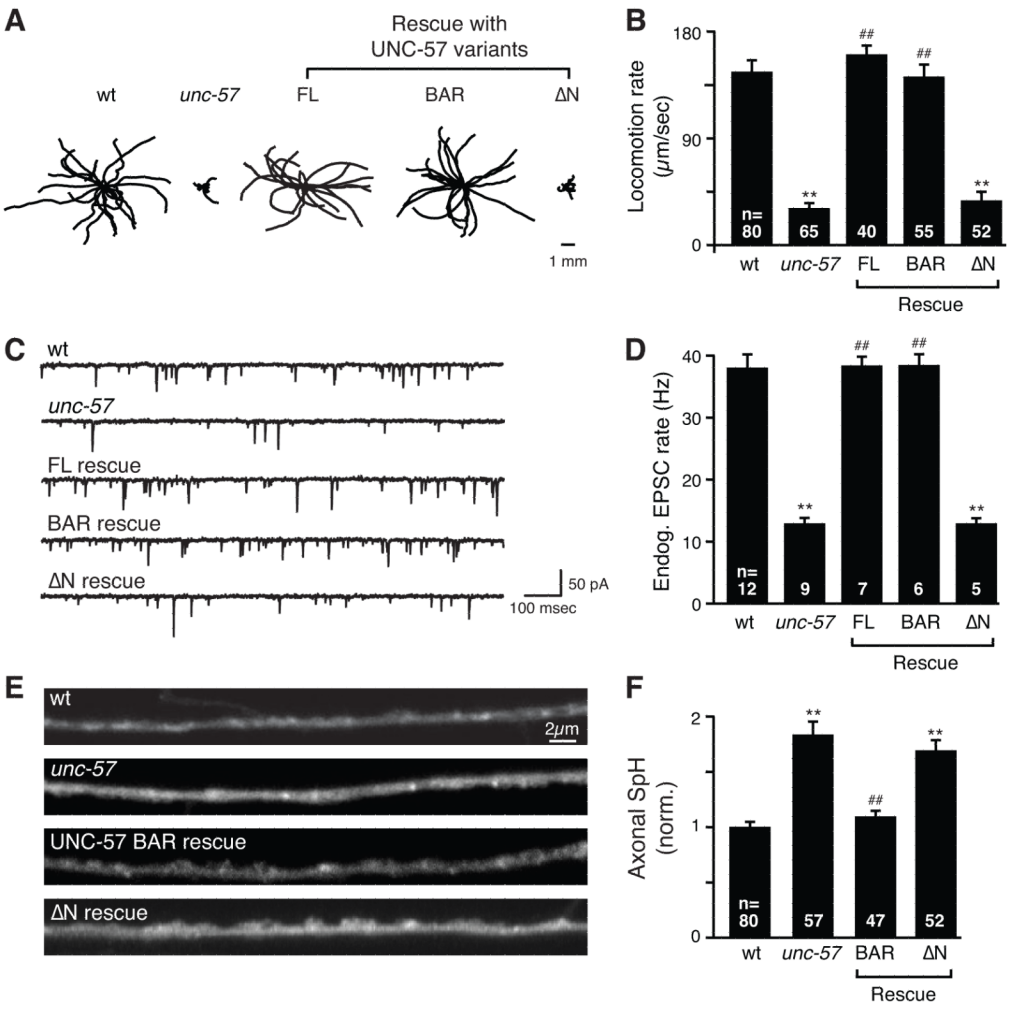

Figure 1. The UNC-57 BAR domain promotes SV endocytosis through its membrane interactions

[See also Figure S1 and S2]

The phenotypes of wild type (wt), *unc-57(e406)* endophilin mutants, and the indicated transgenic strains were compared. Transgenes were mCherry tagged UNC-57 variants including full length (FL; residues 1-379), BAR domain (residues 1-283) and N (residues 27-379). Transgenes were expressed in all neurons, using the *snb-1* promoter. Expression levels of these transgenes are shown in Figure S1.

(A) Representative one minute locomotion trajectories are shown (n= 20 animals for each genotype). The starting points for each trajectory were aligned for clarity. **(B)** Locomotion rates are compared for the indicated genotypes. Representative traces **(C)** and summary data for endogenous EPSC rates **(D)** are shown. Representative images **(E)** and summary data **(F)** for axonal SpH fluorescence in the dorsal nerve cord are shown for the indicated genotypes. The number of worms analyzed for each genotype is indicated. (**) indicates $p < 0.001$ compared to WT controls. ($^{\#\#}$) indicates $p < 0.001$ when compared to *unc-57* mutants. Error bars = SEM.

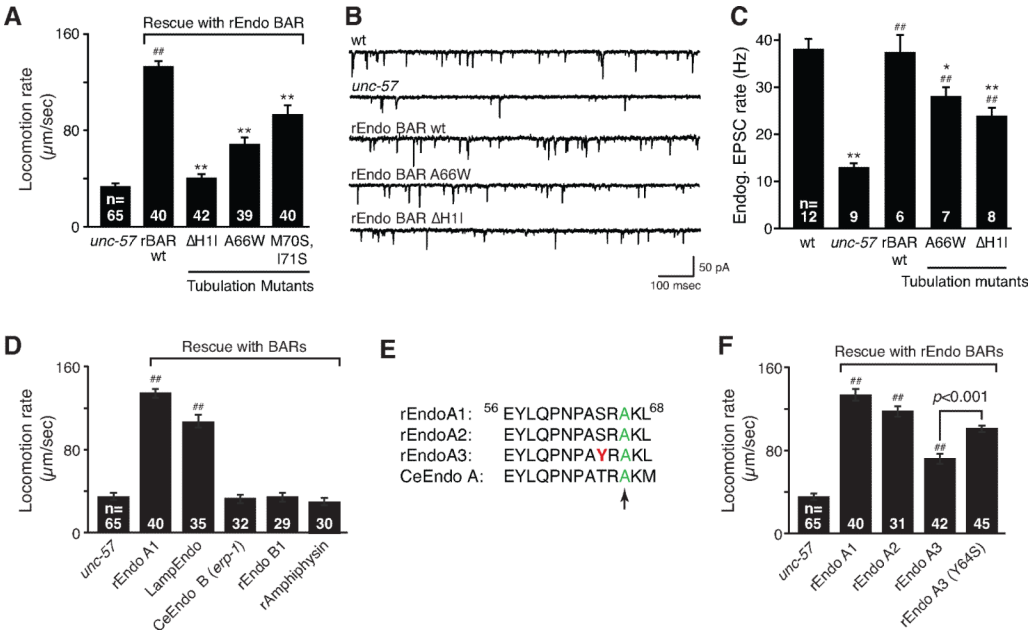

Figure 2. The membrane-bending activity of Endophilin A BAR domains promotes SV endocytosis

[See also Figure S3]

Transgenes encoding wild type and mutant BAR domains (1–247) from rat EndophilinA1 (rEndoA1 BAR) were analyzed for their ability to rescue locomotion rate (**A**), the surface Synaptobrevin (SpH) (Figure S3B) and EPSC rate (**B**–**C**) defects of *unc-57* mutants. The ΔH1, A66W, and M70S/I71S mutations alter membrane tubulation activity but have little or no effect on membrane binding *in vitro* (Gallop et al., 2006; Masuda et al., 2006). All transgenes were tagged with mCherry at the C-terminus to assess differences in expression levels (Figure S3). **(D)** Transgenes expressing BAR domains derived from different proteins were compared for their ability to rescue the locomotion rate defect of *unc-57* mutants. BAR domains are indicated as follows: rat Endophilin A (rEndo A1, A2, and A3; residues 1-247), lamprey Endophilin A (LampEndo; residues 1-248), *C. elegans* (CeEndo B; residues 1-267), rat Endophilin B (rEndo B; residues 1-247), and rat Amphiphysin (rAmphiphysin; residues 1-250). **(E)** Alignment of the H1 helix sequence is shown for the indicated BAR domains. The A66 residue (green, arrow) is required for tubulation activity (Masuda et al., 2006). rEndo A3 has a sequence polymorphism (S64Y) compared to the A1 and A2 isoforms. **(F)** Rescuing activities of rEndo A1, A2, A3, and A3(Y64S) BAR domains for the *unc-57* mutant locomotion defect are compared. All transgenes were expressed in all neurons using the *snb-1* promoter. The number of animals analyzed for each genotype is indicated. (**) and (*) indicate significant differences compared to wt ($p< 0.001$ and $p< 0.01$, respectively). ($^{\#\#}$) indicates $p< 0.001$ when compared to *unc-57* mutants. Error bars = SEM.

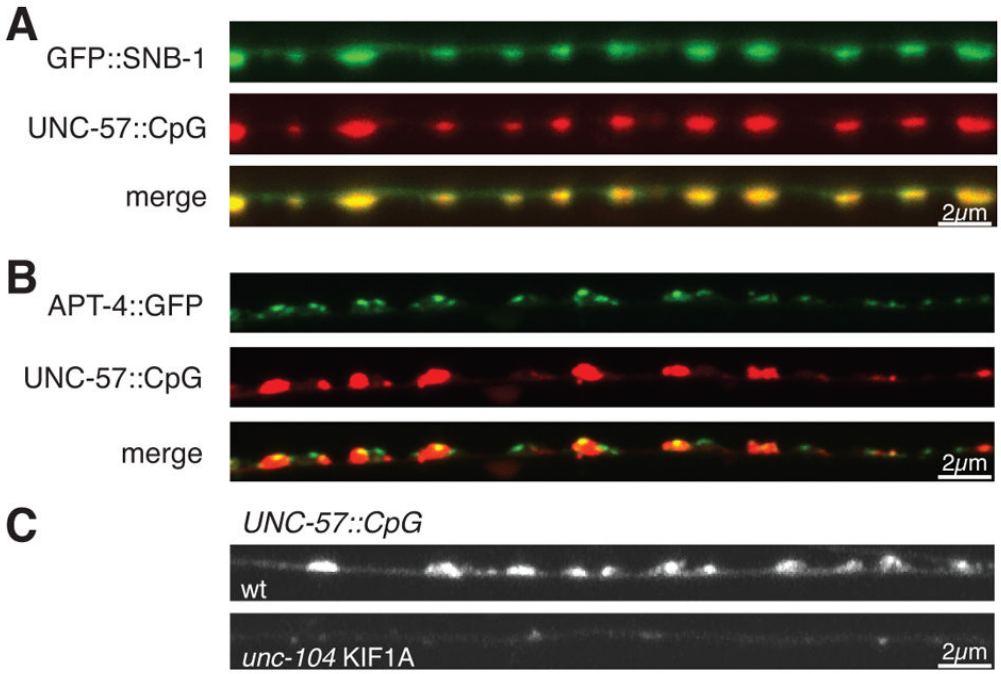

Figure 3. Endophilin is targeted to the SV pool at presynaptic terminals

[See also Figure S4]

Full-length *unc-57* Endophilin was tagged at the C-terminus with mCherry and photoactivatable GFP (designated as CpG) (schematic shown in Fig. 4A). (**A**–**B**) The distribution of UNC-57::CpG mcherry fluorescence in DA neuron dorsal axons is compared with a co-expressed SV (GFP::SNB-1, **A**) or endocytic marker (APT-4::GFP AP2α, **B**). **(C)** Targeting of UNC-57::CpG to presynaptic terminals was strongly reduced in *unc-104(e1265)* KIF1A mutants.

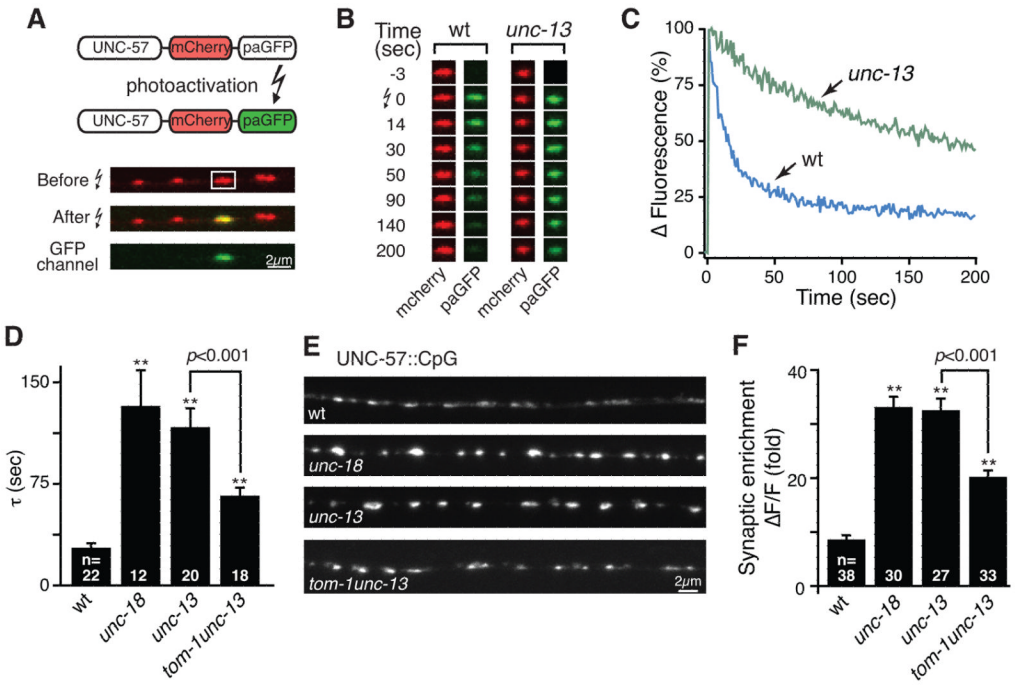

Figure 4. Exocytosis promotes dissociation of Endophilin from the SV pool

[See also Figure S5]

(A). Photoactivation of UNC-57::CpG at a single synapse is shown schematically (above) and in representative images (below). **(B–C)**. Representative images and traces of photoactivated UNC-57::CpG green fluorescence decay in wild type (wt) and *unc-13(s69)* mutants. The mCherry fluorescence was captured to control for motion artifacts. **(D).** Dispersion rates of photoactivated UNC-57::CpG were quantified in the indicated genotypes. Decay constants (τ) are 28.1 ± 3.3 sec for wt; 117.2 ± 13.6 sec for *unc-13 (s69)*; 136.2 ± 26.4 sec for *unc-18 (e81)*; and 68.2 ± 6.5 sec for *tom-1(nu468)unc-13(s69)*. Representative images **(E)** and summary data **(F)** for steady-state UNC-57::CpG mCherry fluorescence in the dorsal nerve cord axons was compared for the indicated genotypes. **(F)** Synaptic enrichment of UNC-57::CpG was calculated as follows: $\Delta F/F = (F_{peak} - F_{axon})/F_{axon}$. The number of animals analyzed for each genotype is indicated. ** indicates $p < 0.001$ compared to wt controls. Error bars = SEM.

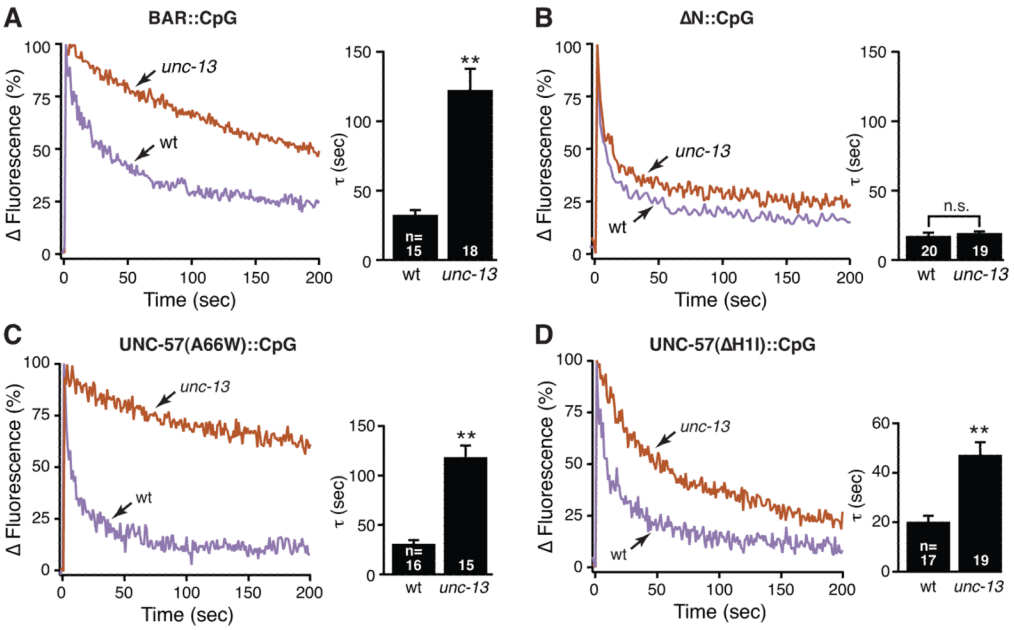

Figure 5. Structural requirements for UNC-57 regulation by exocytosis

[See also Figure S6]

Representative traces and summary data are shown comparing the dispersion of mutant UNC-57 proteins. Mutant proteins analyzed are: **(A)** WT BAR domain lacking the SH3 (BAR reporter), and full length UNC-57 proteins containing the ΔN (membrane binding deficient) **(B)**, A66W (tubulation deficient) **(C)**, and ΔH1I (dimerization deficient) **(D)** mutations. Each mutant protein was tagged with CpG, expressed in DA neurons, and their dispersion rates compared following photoactivation in wild type and *unc-13* mutants. (**) indicates $p < 0.001$ compared to wt controls. Error bars = SEM.

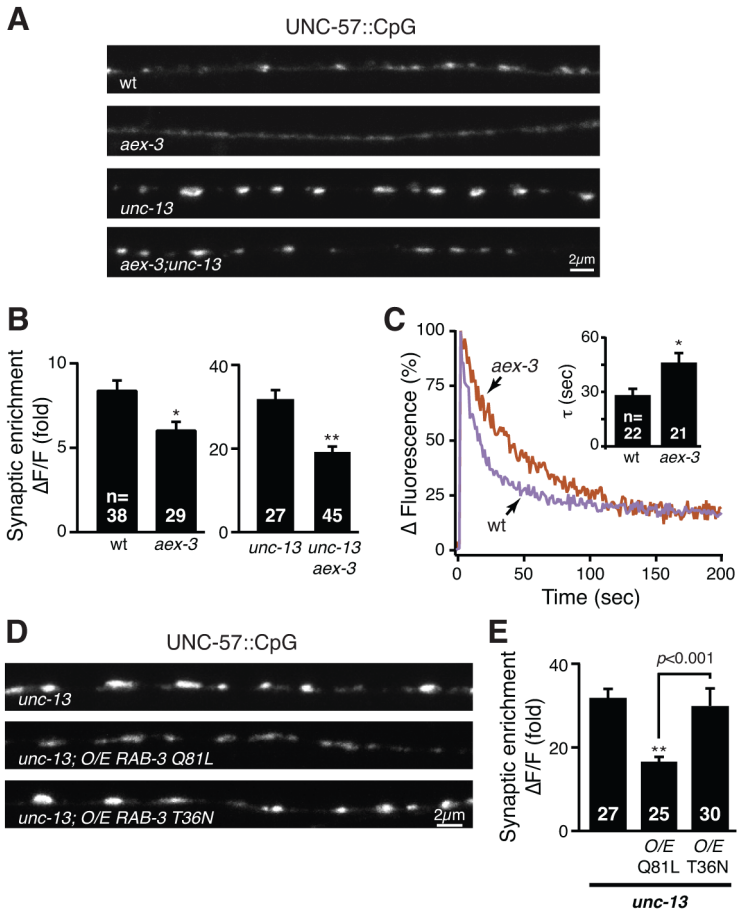

Figure 6. RAB-3 and the Rab3 GEF (AEX-3) regulate Endophilin targeting to SVs

Representative images **(A)** and quantification **(B)** of UNC-57::CpG synaptic enrichment in *wt*, *aex-3*, *unc-13* and *unc-13;aex-3* double mutants were shown (Synaptic enrichment: wt 8.6 ± 0.6; *aex-3* 6.2 ± 0.6; *unc-13; aex-3* 19.6 ± 1.2, *unc-13* 32.1 ± 2.2 fold). Dispersion rates of UNC-57::CpG in wt (τ = 28.1 ± 3.3 sec) and *aex-3* mutant (τ = 45.5 ± 5.1 sec) animals were compared in **(C). (D–E)** UNC-57::CpG distribution in transgenic *unc-13* mutant animals with over-expressed RAB-3 (Q81L) or (T36N) was studied. Over-expression of RAB-3 (Q81L), but not RAB-3 (T36N) significantly reduced UNC-57::CpG synaptic enrichment in *unc-13* mutants. ** indicates p <0.001 and * indicates p <0.01, compared to wt controls. Error bars = SEM.

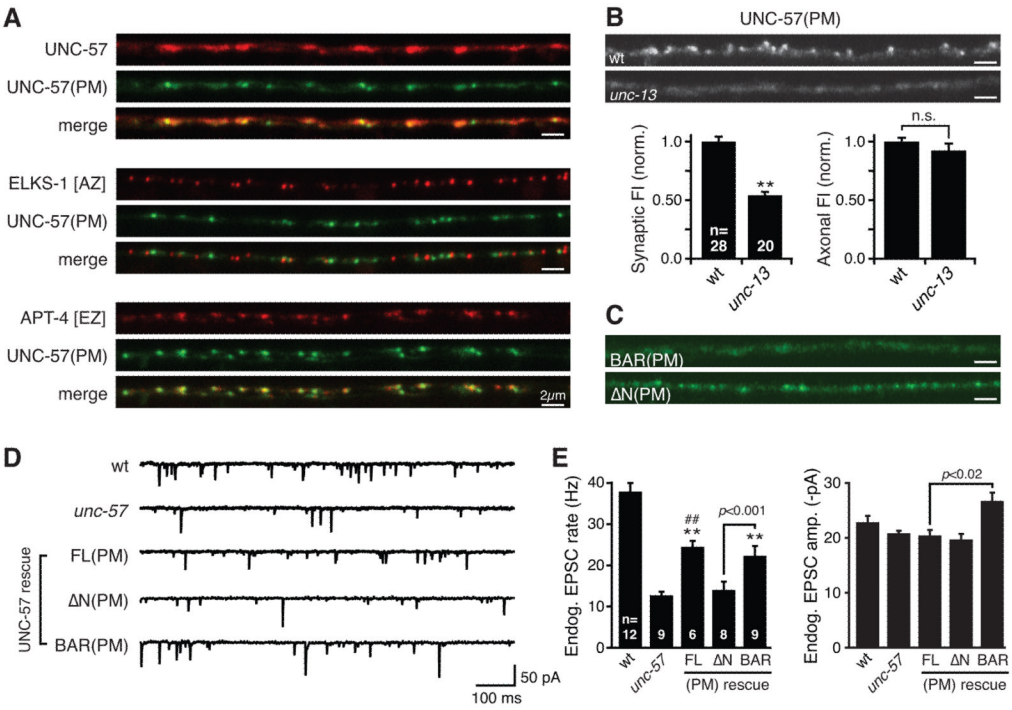

Figure 7. Analysis of a membrane-anchored UNC-57 protein

[See also Figure S7]

(A) The distribution of UNC-57(PM) in DA neuron axons was compared with co-expressed UNC-57::CpG (*upper panels*), active zone [AZ] marker ELKS-1::mcherry (*middle panels*), or endocytic zone [EZ] marker APT-4::mcherry (AP2α, *lower panels*). UNC-57(PM) comprises full length UNC-57 and GFP fused to the N-terminus of UNC-64 Syntaxin 1A (schematic shown in Figure S7A). **(B)** GFP fluorescence of UNC-57(PM) in wt and *unc-13(s69)* mutant animals were quantified. UNC-57(PM) was expressed in all neurons with the *snb-1* promoter. **(C)** Representative images are shown of wild type and mutant UNC-57(PM) proteins in dorsal cord axons. The BAR(PM) protein corresponds to UNC-57(PM) lacking the SH3 domain. The ΔN(PM) protein lacks the N-terminal 26 residues of UNC-57 (which prevents membrane binding). **(D)** Representative traces of endogenous EPSC from wt, *unc-57(e406)* mutants, and transgenic *unc-57* animals carrying wild type and mutant UNC-57(PM) constructs. Endogenous EPSC rates (left panel) and amplitudes (right panel) are shown in **(E).** Significant differences (p <0.001 by student's t-test) are indicated as: **, compared to wt; and ##, compared to *unc-57* mutants. Error bars = SEM.